
FUSED-MEMBRAIN: A SPIKING PROCESSOR COMBINING CMOS AND SELF-ASSEMBLED MEMRISTIVE NETWORKS

Davide Cipollini^{*1,3}, Hugh Greatorex^{*2,3}, Michele Mastella^{2,3}, Elisabetta Chicca^{2,3}, Lambert Schomaker^{1,3}

¹Bernoulli Institute for Mathematics, Computer Science and Artificial Intelligence, University of Groningen, Netherlands

²Bio-Inspired Circuits and Systems (BICS) Lab, Zernike Institute for Advanced Materials, University of Groningen, Netherlands

³Cognigron - Groningen Cognitive Systems and Materials Center, University of Groningen, Netherlands

*Corresponding authors: d.cipollini@rug.nl, h.r.greatorex@rug.nl

ABSTRACT

In an era characterized by the rapid growth of data processing, developing new and efficient data processing technologies has become a priority. We address this by proposing a novel type of neuromorphic technology we call Fused-MemBrain. Our proposal is inspired by Golgi’s theory modeling the brain as a syncytial continuum, in contrast to Cajal’s theory of neurons and synapses being discrete elements. While Cajal’s theory has long been the dominant and experimentally validated view of the nervous system, recent discoveries showed that a species of marine invertebrate (ctenophore *Mnemiopsis leidyi*) may be better described by Golgi’s theory. The core idea is to develop hardware that functions analogously to a syncytial network, exploiting self-assembled memristive systems and combining them with CMOS technologies, interfacing with the silicon back-end-of-line. In this way, a memristive self-assembled material can cheaply and efficiently replace the synaptic connections between CMOS neuron implementations in neuromorphic hardware, enhancing the capability of massively parallel computation. The fusion of CMOS circuits with a memristive “plexus” allows information transfer without requiring engineered synapses, which typically consume significant area. As the first step toward this ambitious goal, we present a simulation of a memristive network interfaced with spiking neural networks. Additionally, we describe the potential benefits of such a system, along with key technical aspects it should incorporate.

Keywords neuromorphic computing · spiking neural networks · memristive networks · in-memory computing · back-end of line integration

1 Introduction

Artificial information processing has already become one of the main contributors to the current climate and energy crisis [2]. Vast amounts of data are continuously generated and fed into our computing machines. Moreover, sophisticated AI tools, such as Large Language Models, are currently over-utilized to handle even the simplest tasks, largely due to their public and nearly limitless availability [2]. While chip manufacturing companies strive to find new solutions to continue the miniaturization of integrated circuits, the physical limitations are dawning upon them [3]. With this on the horizon, emerging and specialized computing schemes are poised to become viable solutions, particularly when integrated with developing devices and materials.

Neuromorphic engineering [4, 5] takes inspiration from the remarkable energy efficiency of the brain [6] and leverages the physics of devices such as transistors to mimic the dynamical behavior of neural circuits. Often, the field grapples with the challenge of achieving reliable computation from unreliable computational elements [7], in contrast to modern digital signal processing circuits designed to be robust to noise. In stark contrast, brain function is underpinned by billions of neurons and trillions of synapses and dendrites communicating via analog (potentials) and digital signals (spikes). The biological computing paradigm is inherently stochastic, redundant, and resilient to noise and individual defects, standing in bold relief against the backdrop of modern digital computing. Neuromorphic computing and engineering endeavor to remove, or at least minimize, the physical distance between CPU and memory,

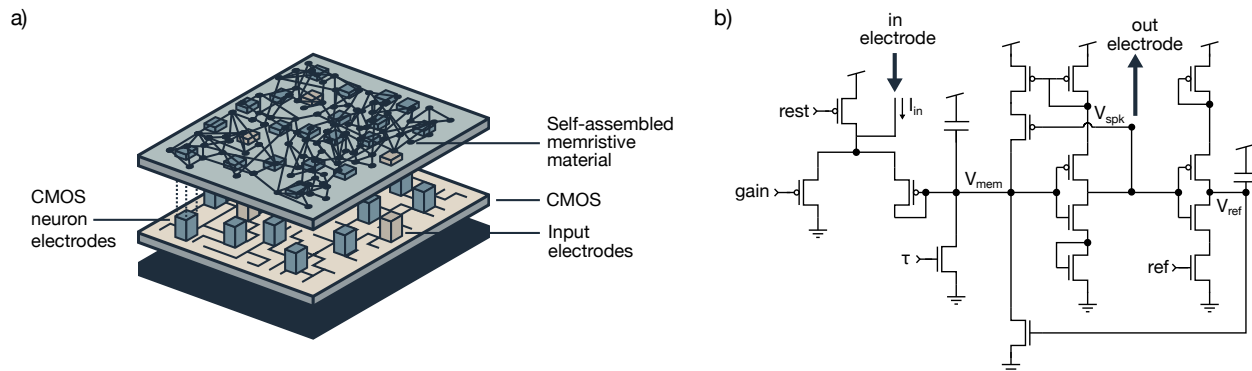


Fig. 1: **The proposed Fused-MemBrain processor.** **a)** A schematic depiction of the proposed hardware. A CMOS layer contains all of the neuron circuitry and configuration. On top, a self-assembled memristive material is deposited. The interfacing of the two layers is facilitated by electrodes protruding from the uppermost layers of Complementary Metal Oxide Semiconductor (CMOS). **b)** an exemplary neuron circuit adapted from [1]. The neuron integrates input currents from the plexus through one of its two electrodes (in electrode). Once the neuron’s membrane voltage crosses its firing threshold, it generates and transmits a voltage pulse (spike). This pulse can be fed back into the plexus via another electrode (out electrode), stimulating recurrent network activity.

widely referred to as the infamous von Neumann bottleneck. In this way, such hardware functions as a *network-that-does* as much as the brain is, enabling higher bandwidth and significantly reduced energy consumption [8].

The brain possesses an in-homogeneous topological organization [9, 10] in both its structural and functional wiring. This has a profound impact on its activity and its capabilities, so much so that abnormal structures lead to neuropsychiatric pathologies such as schizophrenia [11, 12], epilepsy [13], and attention-deficit/hyperactivity disorder [14]. Moreover, the brain functions as a spatial network [15], with nodes positioned in physical space and a topological structure shaped by physical constraints and resource limitations [16].

Many of these properties are not realized when cross-bar arrays of analog memristive memories are used to implement efficient in-memory computation. Cross-bar arrays operate to accelerate the matrix-vector multiplications at the foundation of artificial neural network algorithms, nevertheless, they become inefficient when recurrent dynamics are imposed, especially when matrices reflecting the coupling between elements are sparse off-diagonal. The realization of specialized hardware for small-world connectivity has been addressed [17] requiring the shrewd top-down design of pairwise memristive synapses given specific properties of the wiring topology. Nevertheless, the bottom-up realization of self-assembled memristive materials [18] may allow the efficient, reconfigurable, and almost designless realization of multielectrode devices with the significant advantage of reducing the area the CMOS-synapses consume in hardware.

We propose making use of the memristive disordered topology of in-organic materials to implement the coupling, and conventional analog and digital electronics to implement the activity of the nodes. We note that previous studies in the literature have demonstrated high-density multielectrode arrays integrated with disordered wetware with *in-*

silico computing [19–21]. *In vitro* neurons embedded in high-density electrodes are already under consideration to harness the computational power of biological systems, and the self-adaption of their neural response to the environment upon free energy minimization has been demonstrated [22]. We present a similar multi-electrode system exploiting inorganic materials, provide an easy-to-use simulator for experimentation, and examine the potential implications of the proposed hardware.

Therefore the main contribution of this work is twofold:

1. The proposal for a spiking system equivalent to a syncytial network on hardware.
2. The development of a compact simulator complementary to this proposal.

2 Fused network and the biological neuron doctrine

One of the most significant technical advances in the investigation of the nervous system was the so-called “black reaction” method, invented by Camillo Golgi in the 19th century [23]. With this new technique, Golgi could stain a small percentage of the elements within a block of nervous tissue. This enabled the visualization of entire nerve cells, including their dendritic arborization and axons, using a microscope [24]. As a result of his experimental work, Golgi proposed his theory, suggesting that the nervous system was a *syncytial continuum*. According to his hypothesis, nerve cells were fused into a single giant membrane, forming a *plexus* that served as the primary integrative structure of the nervous system. Around the same time, another celebrated scientist, Santiago Ramón y Cajal, adopted the black-reaction technique that Golgi pioneered. Opposing the fused network theory of his contemporary, Cajal hypothesized that the nervous system was composed of discrete elements, called neurons, that may interface

with one another but never fuse. Although both Golgi and Cajal won the Nobel Prize in Physiology or Medicine in 1906, the advent of electron microscopy, which enabled the discovery of synaptic connections between individual neurons [25, 26], ultimately led to the rejection of Golgi’s theory in favor of the neuron doctrine proposed by Cajal.

However, there is some increasing evidence that for some jellyfish, such as the ctenophore *Mnemiopsis leidyi*, nerve-net neurons connect through a syncytial continuum: a wide network extending from only one soma [27]. This type of architecture may be appropriate if its main function is to display sensitivity for the relevant dynamics at the input (sensor) and have the required dynamical properties towards the output (actuator), i.e., general locomotion for foraging/oxygen intake and predator evasion, in the case of jellyfish, with its typical sensory reactivity and contractile reactions [28].

In this work, we aim to propose and explore the possibilities of a comparable self-assembled, self-organized memristive spiking network in hardware, not as a replacement for other forms of neural processing, but as a complementary approach characterized by architectural simplicity while still being capable of handling the required non-linear dynamics of the associated real-world functions [29, 30].

3 Fused-MemBrain: Hardware

The proposed hardware is defined as combining two main components. The first component is an ensemble of CMOS neurons, e.g. Leaky Integrate and Fire (LIF) equipped with two electrodes: one that sources currents and one that provides voltage. The *in* electrode drains the electrical current from its surroundings, integrates it, and produces a voltage that the *out* electrode applies back into the plexus. Such CMOS neurons are configurable and the external user can set their dynamical parameters to the requirements imposed by the task.

The second component is the self-assembled memristive plexus deposited on the silicon back-end-of-line which couples the neuron electrodes. Thus, signals between coupled neurons are wave-like propagated *in materio* through time and the physical space.

The emerging field of self-assembled neuromorphic materials [18, 31], e.g. nanowire networks [31–33], domain wall networks [34], nanocluster-assembled devices [35, 36], disordered dopant-atom network [37], disordered networks of nanodots [38, 39] present themselves as promising candidates to replace the synaptic circuitry. The deposition of many of these materials, e.g. nanowires, nanodots, and nanocluster assemblies, being CMOS-compatible, can in principle be interfaced with the circuitry on the silicon back-end-of-line [40], providing an efficient and low-cost solution to signal routing across the ensemble of CMOS neurons. They can be used to reduce the area required for realizing synaptic circuitry, thus reducing the silicon real

estate, while at the same time enhancing the capability of massively parallel computation for *in-materio* computing.

Fig. 1 schematizes the envisioned Fused-MemBrain hardware realization. The dynamic behavior of the self-assembled memristive material can, in principle, be exploited to implement short- or long-term plasticity between the neurons, which could realize self-healing and self-organizing recurrent dynamical systems.

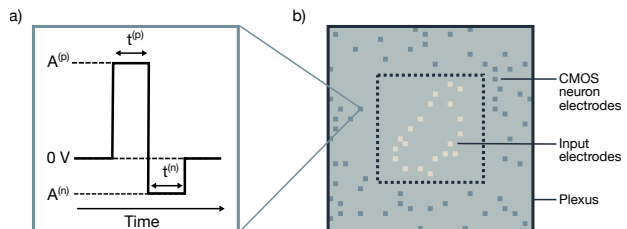


Fig. 2: **CMOS neuron configuration.** **a)** The spike-pulse shape is illustrated. **b)** Input nodes are located in the central region of the plexus delimited by the square perimeter. They inject the input data and drive the system out of equilibrium. They are disposed to reflect the 20 higher-intensity coarse-grained pixels of a zero-digit sample from the MNIST dataset.

3.1 Configuration of the CMOS neurons

3.1.1 Spike shapes for synaptic and heterosynaptic plasticity

The spike pulse, applied by the neurons onto the plexus, was engineered to be compatible with the electrical properties of the self-assembled material. Spikes are simplified as a positive square voltage followed by a negative square voltage as depicted in Fig. 2a, mimicking the biological alternation between the spike and the refractory period. The amplitudes, $A^{(p)}$ and $A^{(n)}$, and the time widths of both the positive and negative square signals, $t^{(p)}$, $t^{(n)}$, are tunable parameters that determine the time-dependent behavior of the overall system. The voltage difference between different neurons, generated by the shape of the spike (first positive, then negative), enables causal dependence between the spiking activity between two neurons in the same physical neighborhood. Let us take two neurons on the plexus, where one has entered the refractory period, $t^{(n)}$ and the other is currently applying the positive voltage, $A^{(p)}$, the voltage difference applied to the memristive plexus is the highest possible $\Delta V = A^{(p)} - A^{(n)}$ producing the enhancement of conductive pathways between these two electrodes resembling the synaptic plasticity.

3.1.2 Electrode spatial distribution

The Fused-MemBrain hardware enables the deployment of multiple electrodes, unlike the simpler utilizing only two electrodes case as described in Ref. [41], as a result, the voltage landscape over the plexus is significantly more complex. Since the synaptic plexus, rather than discrete connections between individual neuron pairs, real-

izes higher-order coupling, any change in coupling efficacy between one neuron pair will also influence the efficacy between other pairs, similar to heterosynaptic plasticity [42]. Therefore, given that there is no direct access to the connections between neurons and that the connections are of high order, we lose direct control of the synaptic connectivity and rely solely on the self-organization of the conductive memristive material. However, we retain control of the parameters governing the dynamics of the CMOS neurons along with their distribution on the plexus. See the last column of Table 2. This is an alternative and tangible way to modify the spatiotemporal behavior of the plexus.

In Fig. 2b, we show an example distribution of the electrodes across the plexus. We categorize the electrodes protruding into the memristive plexus as *input* electrodes and the electrodes of the CMOS neurons. The input electrodes are located within the central region of the processor, indicated by the inner square in panel Fig. 2b. These electrodes are used to inject the input signals and do not interact with the plexus after the presentation of the sample. As an example (Fig. 2) the input electrodes are placed to reflect the location of the active pixels of a zero-digit sample from the MNIST dataset. The green squares indicate the distribution of the CMOS neurons.

Speculatively, an intriguing extension could involve introducing quantum dots into the input electrode region of the memristive plexus. Thus, optical input signals encoding data could be efficiently converted into electrical signals propagating to the neuron-electrodes and initiating their activity [38, 39].

4 Fused-MemBrain: Simulator

The numerical simulation of the Fused-MemBrain hardware is implemented through the Modified Voltage Nodal Analysis (MVNA) [43] formalism used in SPICE-type simulators for electronic circuits [44]. MVNA solves for the currents flowing into the sources and the voltages over each node in the network describing the plexus. At each time step, the system is simulated according to the pseudo-code described in Section 4.4 where neurons and the plexus interact dynamically. The implementation of the memristive plexus is based on [41], in which the simulator from [45] was adapted to take advantage of sparse matrices thanks to the planar nature of the system, therefore reducing simulation time. The simulation of the interface between CMOS neurons and the self-assembled memristive network is an original contribution of this work.

4.1 Coarse-graining the plexus

To model the plexus, we aggregate the conductive properties of the self-assembled memristive material deposited on the back-end-of-line. We tile the plexus in equivalent square regions of $\simeq 25 \mu\text{m}$ linear size equal to the expected unit size of a single CMOS neuron [40], which becomes our unit scale in space. In network terminology, a node is

defined as the representative of each region of the plexus and is coupled to the adjacent nodes by an edge. The topological properties are held simple under the assumption of grid-graph structural connectivity with non-overlapping random diagonal edges to preserve the device’s planar dimensionality. In other words, the conductive properties of the material between two coarse-grained region centers are aggregated and a memristor model is associated with each dynamical edge in the network governing the conductivity level encoded in its weight. A similar scheme was originally proposed in Ref. [33, 45] to model conductive networks of nanowires.

Note that this coarse-graining approach allows the higher-order interactions between CMOS neurons that would otherwise be lost if we modeled the system as a pairwise interaction network. Moreover, space and time retain a role in signal propagation delays. Delays depend on the dynamical model and the time constants of the memristor model, i.e. the edge connecting two neighboring regions in our model, as well as the space the signal needs to traverse.

4.2 Memristor model

The voltage-driven dynamic of a single memristive edge connecting two coarse-grained regions of the plexus is captured by the model originally proposed for nanowire networks [33, 45, 46] exhibiting Short Term Plasticity (STP) effects including potentiation, depression and relaxation, paired-pulse-facilitation [47], as well as heterosynaptic plasticity. The memristor model is based on the following potentiation-depression rate balance equation:

$$\frac{dg}{dt} = (1 - g)k_p(V) - gk_d(V) \quad (1)$$

where $0 \leq g \leq 1$ is the normalized conductance and k_p , k_d are the potentiation and depression rate coefficients. For simplicity, they are assumed to depend exponentially only on the absolute voltage difference between two neighboring regions and account for the physical ionic diffusion [46, 48–50]:

$$k_{p,d}(V) = k_{p0,d0}e^{\pm\eta_{p,d}|V|} \quad (2)$$

where $+$ and $-$ are associated with k_p and k_d respectively. $k_{p0,d0} > 0$ are fitting constants and $\eta_{p,d} > 0$ are transition rates.

The current flowing through each edge is assumed to follow Ohm’s law for electrical transport:

$$I(t) = [g(t)G_{\max} + (1 - g(t))G_{\min}]V(t) \quad (3)$$

where G_{\min} and G_{\max} are the minimum and maximum values of the conductance, respectively. These conductance values need to be empirically identified according to the physical memristive material used for the actual physical implementation of the Fused-MemBrain hardware. To develop the empirical realization of the hardware, a more useful and practical quantity would be the conductivity, i.e. the conductance per coarse-grained unit length. Specifically, it would be convenient to use an (edge) conductivity

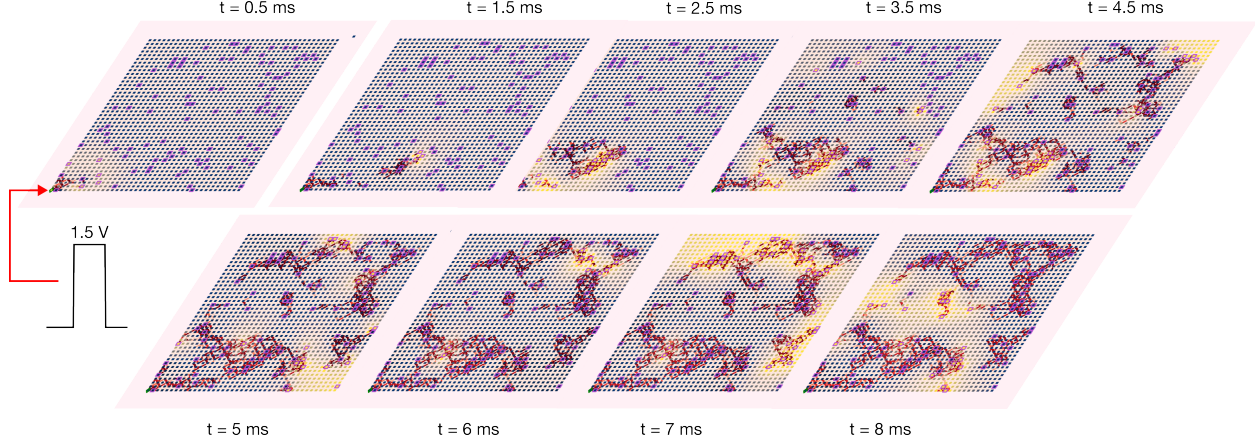


Fig. 3: **Signal propagation through the memristive plexus across space and time.** A voltage pulse of magnitude 1.5 V and width of 1 ms is applied through an input electrode at the bottom left corner of the plexus indicated by the red arrow. The signal propagates through the planar system of memristively-coupled CMOS neurons (depicted by the purple squares). The activation pulse is sufficient to initiate the neurons’ self-sustained activity. Note how the conductance distribution (red edges) is shaped by the activity of the network, producing clusters in regions with a higher density of CMOS neurons. The size of the simulated system is $1025 \mu\text{m} \times 1025 \mu\text{m}$.

$\sigma_* = G_*/l$ over the fundamental length, $l = 25 \mu\text{m}$, defined in the coarse-graining by the CMOS neuron linear size in Section 4.2.

The advantage of the memristor model of Equations (1) and (2) is the low computational cost due to the analytical solution available for discrete time steps $\Delta t > 0$:

$$g(t + \Delta t) = \tilde{g}(1 - e^{-\theta\Delta t}) + g(t)e^{-\theta\Delta t} \quad (4)$$

where $\tilde{g}(V) = \frac{k_p}{k_p + k_d}$ is the dynamic attractor of the memristive network [51, 52]. In other words, \tilde{g} is the final state of the memristive plexus for a given applied voltage. Note that such a final state is independent of the initial conductance state. The exponent $\theta = k_p + k_d$ modulates the speed of reversion and it also depends only on the voltage. The model has 6 parameters summarized in Table 1 plus an extra parameter that sets the edge pristine conductance.

As a final remark, for edges that do not show memristive properties but only linear electrical conduction, Equations (3) and (4) reduce to $g \simeq 0$ and $I(t) \simeq G_{\min}V(t)$, respectively. The possibility of setting a uniform distribution of Ohmic edges is included in the simulator settings. Moreover, our simulator design’s modularity and extensibility allow for the easy substitution of distinct memristor models within our simulation scheme, important for comparing and prototyping different self-assembled materials.

4.3 Spiking neuron model

We model and approximate the deterministic CMOS neuron dynamics with the lifLIF neuron model proposed by Lapicque [53]:

$$\frac{dV_m}{dt} = -\frac{V_m}{\tau_m} + \frac{I_{\text{ext}}}{C_m} \quad (5)$$

V_m is the membrane potential, τ_m is the membrane time constant, C_m is the membrane capacitance, and the I_{ext} is the external current inflow from the memristive plexus to the CMOS neuron input electrode. We approximate Equation (5) with the discrete update rule with exponential decay:

$$V_m(t + \Delta t) = V_m(t)e^{-\Delta t/\tau_m} + \frac{I_{\text{ext}}(t)}{C_m}\Delta t \quad (6)$$

When the neuron’s membrane potential reaches the spike threshold, V^{th} , it spikes and applies a voltage pulse to the plexus of the type illustrated in panel (a) of Fig. 2. This pulse is parametrized by the positive and negative pulse widths, $t^{(p)}$, $t^{(n)}$, and the positive and negative amplitudes, $A^{(p)}$, $A^{(n)}$. Immediately after the spike, the membrane potential is reset to $V_m = 0$ and the neuron enters its refractory period for a time equal to $t^{(n)}$. Table 2 summarizes the parameters of the CMOS LIF model used in our simulations. More complex neuron models could, of course, also be implemented; however, the LIF neuron model is sufficient as a framework for future CMOS implementations and investigations into the behavior of this type of hardware.

4.4 Simulator algorithm

The following algorithm defines how the Fused-MemBrain simulator is both initialized and executed:

1. Initialize the plexus with the conductance distribution over the edges.
2. Set the electrode’s location. Place input electrodes and neurons.
3. Provide the input signal that will drive the network out of equilibrium.

Parameter	Description	Units	Value
k_{p0}	Potential fitting constant	s^{-1}	$2.56 \mu s^{-1} (\times 10^{-6} s^{-1})$
k_{d0}	Depression fitting constant	s^{-1}	$64.90 s^{-1}$
η_p	Potential transition rate	V^{-1}	$34.90 V^{-1}$
η_d	Depression transition rate	V^{-1}	$5.59 V^{-1}$
G_{max}	Maximum conductance	S	200 pS (200×10^{-12} S)
G_{min}	Minimum conductance	S	1 pS (1×10^{-12} S)

Table 1: **Parameters of the memristor model.** k_{p0} , k_{d0} , η_p , η_d values are from Ref. [33]. In Ref. [33], $G_{min} = 1.01$ mS, $G_{max} = 2.72$ mS. Here they are adapted to obtain suitable values $I_{ext} \simeq 10$ pA currents compatible with the CMOS neurons according to the relation $I_{ext} \sim (G_{max} - G_{min}) \cdot (A^{(p)} - A^{(n)})$. Note that in Ref. [33], G_{min} , G_{max} are effective values measured for a specific configuration of electrodes.

Parameter	Description	Units	Typical CMOS value	Simulation value	Tunable
τ_m	Membrane time constant	s	10 - 100 ms	1 ms	✓
I_{ext}	External current inflow	A	[10 pA, 1 nA]	$\sim 1 \times 10^{-10}$ A	NA
V^{th}	Voltage threshold for neuron spike	V	[0.5, 0.9] V	0.5 V	✓
$t^{(p)}$	Positive pulse width (spike)	s	-	0.50 ms (5×10^{-4} s)	✓
$t^{(n)}$	Negative pulse width (refractory)	s	-	0.3 ms (3×10^{-4} s)	✓
$A^{(p)}$	Positive pulse amplitude (spike)	V	[0.5, 2] V	1.2 V	✓
$A^{(n)}$	Negative pulse amplitude (refractory)	V	[-0.5, -0.1] V	-0.1 V	✓
V_m	Membrane potential	V	[0, V^{th}] V	[0, V^{th}] V	NA
$C_m/\Delta t$	Membrane capacitance	F/s	-	3.5×10^{-20} F/s	✗
Δt	Discrete time step	s	-	0.1 ms (0.0001 s)	NA

Table 2: **Parameters of the CMOS LIF neuron model.** The last column indicates the tunable parameters, which thus provide a mean of control over the dynamical behavior of the overall system, and their possible exploitation in learning.

At each time step:

1. Identify the neurons that have reached their spiking threshold and prime the voltage pulse that will be applied to the plexus at the next time step.
2. Apply the voltages computed before and those of the input electrodes and solve the voltage distribution and the current flowing over the plexus.
3. Update the edge conductances according to the memristor model and the resolved voltage distribution.
4. Update the membrane potential of the CMOS neurons based on the in-flowing currents or reset it to the baseline if the neuron produced a spike.

4.5 Example dynamical regime

In Fig. 4, we stimulate the network with a 1.5 V pulse of 1 μ s injected at the bottom left corner indicated by the red arrow in Fig. 3. The neuron’s spiking activity is illustrated in Fig. 4a. Note the abrupt shift from an initial dense firing activity to one much sparser. The top inset on the right of Fig. 4a shows the initial firing activity propagating as a wavefront from the nodes closer to the input location which then spreads to the rest of the network through time and space. The neuron’s firing activity is sustaining and is drawn into the basin of a dynamical attractor state, illustrated in the bottom inset of panel Fig. 4a. Modules of recurrent high-conductive pathways form in the memris-

tive plexus and stabilize after a transient. This is evidenced by the direct observation of insets of Fig. 3 along with Fig. 4b. The latter shows the average conductance over the memristive edges in time depicting the interplay between the memristive plexus and the firing rates of the CMOS neurons. Fig. 4b shows the average spiking activity of the network starting at high frequency to then relaxing to a lower firing rate. In Fig. 4d, the voltage signal applied to the plexus by the 0-th CMOS neuron is depicted.

This example demonstrates one possible dynamical regime of the simulator, achieved by tuning neuron parameters and their spatial arrangement. A potential use case for this regime could be pattern storage, represented by distinct firing activities across the network, bearing a strong resemblance to attractor networks [54–56].

5 Discussion

Typically, synapses in neuromorphic hardware systems are made of CMOS elements as much as the neurons. Consequently, their design and fabrication require considerable engineering effort because of their bottom-up design. Moreover, the realization of synapses is usually responsible for high power consumption and significant area overhead [57]. In most networks that neuromorphic hardware aims to emulate, the number of synapses scales quadratically with the number of neurons [58], making synapses the primary contributor to the cost of fabrication. Within this work, we envision a potential solution to this

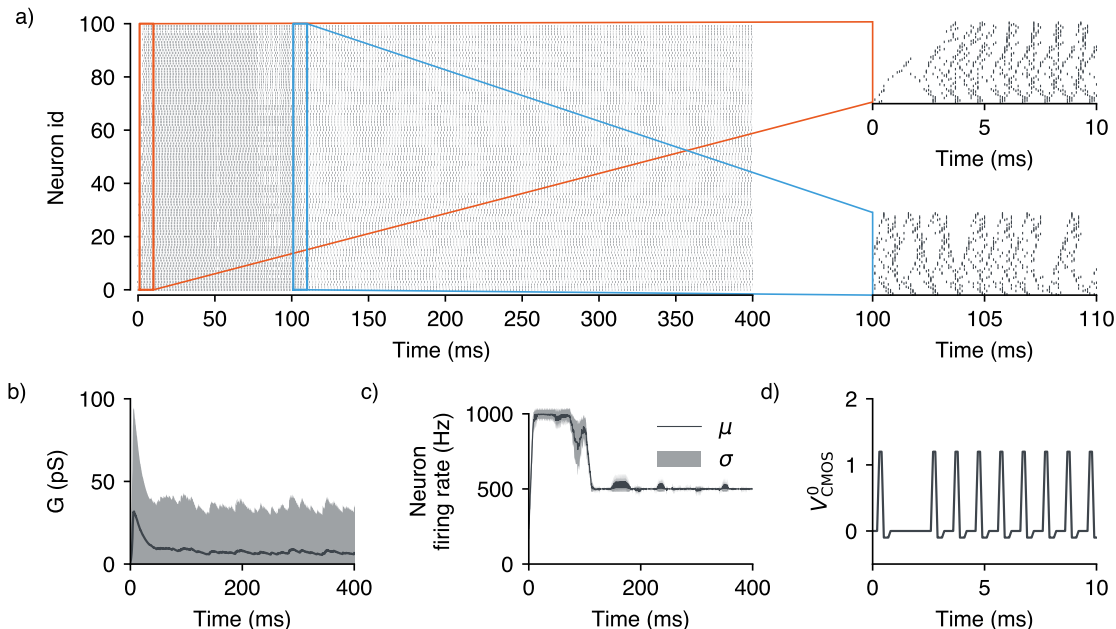


Fig. 4: **Example network activity.** **a)** The firing activity of the CMOS neurons. The top inset depicts the initial propagation of the activity, while the bottom inset depicts the activity at a later time. **b)** The self-sustained neural activity raises the average conductivity from the initial pristine value of the plexus. **c)** The average firing rate of the neurons in the network. **d)** The voltage that neuron 0 applies to the plexus. The neuron begins firing early as it is located close to the origin of the activation signal (bottom left corner of the plexus).

problem by endowing neuromorphic hardware with the power of self-assembled memristive materials [18] that act as a connectivity matrix.

Understanding and controlling the type of dynamics this system can express is crucial for designing neuromorphic hardware capable of solving tasks. To this end, we developed a compact open-source simulator (see Code availability) that can be easily used to identify the working conditions in terms of neuron parameters, electrode locations, and compact device models to finally investigate the compatibility of self-assembled materials in combination with CMOS neuron implementations.

5.1 Physical embedding and higher-order interactions

Neurons communicate with the plexus using digital bipolar pulses as shown in panel Fig. 2a. The memristive material (plexus) converts these pulses into currents flowing around the self-assembled network which are sourced into the electrodes of the CMOS neurons. The plexus mediates the interactions between neurons, which may not necessarily be pairwise [17]. In this system, conductive traces are confined in the 2D embedding space shared between the CMOS neurons, potentially leading to higher order correlations in the activity compared to a network constrained to pair-wise connections. Moreover, this influences the emergence of possible topological traits, such as modules and clusters, self-organized by the activity above the CMOS. Networks, where connections between nodes

incur a cost for spanning physical distances, tend to exhibit higher clustering and fewer high-degree nodes. This pattern arises as a natural consequence of their Euclidean embedding [59–61]. Similarly, the physical structure of the brain [16] constrains its network topology, resulting in a clustered organization with few long-range connections, yet it displays remarkable computation power. Whether this computational efficiency is a direct outcome of these constraints remains an open and interesting question. With this in mind, it makes sense to explore hardware that embraces the physical constraints instead of attempting to circumvent them with costly and challenging connectivity infrastructures. Such hardware could be more economically feasible and cheaper to engineer while still benefiting from high-performance information processing.

5.2 Pathways for system use

An open question raised in this paper is how to effectively utilize such a system. We explore several potential approaches and discuss a selection of them below.

A typical approach would be to use the reservoir computing paradigm, also known as echo-state networks [62] or Liquid State Machines (LSMs) (when units are spiking) [63]. The widely adopted interest in these networks is due to their simplicity and ability to tame dynamical systems into performing useful computation. Only the weights connecting the recursive and output layers need to be learned, usually employing a Support Vector Machine (SVM) or an Multi Layer Perceptron (MLP). To effectively

use the Fused-MemBrain hardware within this context, the temporal behavior of the system needs to be compatible with that of the input data. Therefore, the firing activity of the hardware neurons should be tuned such that the overall system exhibits a decaying behavior after being driven out of equilibrium with the input data. Similar to reservoir computing, Henseler and Braspenning [64] used the differential equations describing the dynamics of a two-dimensional sheet (called “membrain”) to generate moving waves under an input signal perturbation. The “membrain” dynamics were then used as the input for a linear classifier to solve a recognition task. This closely resembles the dynamics observed in our proposed system, as depicted in Fig. 3.

In comparison to the reservoir scheme, where the activity is in the decaying regime, another possibility is to use the system in the *self-sustained* regime as shown in Fig. 4. In this operation mode, learning could be achieved by “structuring” the waves to be pattern-dependent leveraging the Hebbian-like plasticity expressed by the memristive plexus.

In recent work [19–21] *in vitro* biological networks coupled with a multi-electrode array were able to demonstrate “learning” in the context of a closed-loop system. Their experimental setup bears resemblance to the system proposed in this work, in which a high-density network (the plexus) is interfaced with a high-density electrode array (CMOS neurons). How to exhibit a similar demonstration with the Fused-MemBrain hardware depends on the properties of the memristive material used in the physical realization. For instance, when the plexus shows memristive volatile behavior the main control we have over the system dynamics are the neuron parameters, input electrodes, and their locations on the plexus. The volatility of the plexus does not allow for the retention of connectivity structures imperative for a given task, any change in conductivity, and therefore network connectivity, will be lost as the system has an inertia to remain in its pristine state. However, such volatile dynamics remain useful to route signals between neurons. The neurons can be tuned by changing their parameters to impose desired wave patterns within the system. Learning would then be achieved by the dynamics of the neurons existing on multiple time scales as well as their spatial inhomogeneity. As an example, this could be implemented by ensuring neuron activity aligns with the timescales exhibited by the plexus, maintaining an elevated connectivity state and preventing it from completely relaxing.

Alternatively, should the plexus show non-volatile behavior we can design the inhomogeneity of its conductive properties externally, sending the desired signals to write or erase any high-conductivity trace formation in the plexus. This is similar to the approach adopted in Ref. [65] where a physical wave system was trained to learn complex features in temporal data. They demonstrated the classification of audio signals using waveform scattering and propagation through an inhomogeneous medium. For the Fused-

MemBrain hardware to exploit this scheme it would be necessary that the neuron activity is tuned such that it does not override the engineered inhomogeneity.

6 Conclusions

In this paper, we proposed a novel type of neuromorphic hardware that marries the high-density connectivity of self-assembled memristive systems with the versatility and maturity of CMOS technology. The architectural simplicity of our proposal relies on the memristive self-assembled material replacing the synaptic connections between CMOS neurons in the hardware. Synaptic connections are accountable for much of the silicon real estate and therefore the economic cost of neuromorphic hardware. Replacing synapses with a memristive plexus, i.e. a planar sheet of self-assembled memristive elements, with which CMOS neurons are interfaced, could offer a low-cost solution to signal routing. The proposed hardware enables the exploration of emerging self-assembled materials interfacing with a high density of electrodes. Simultaneously it offers a platform to investigate spiking neural network topologies that support higher-order interactions, akin to those observed in biological systems. To pave the way, we developed an open-access simulator to evaluate the compatibility of self-assembled materials with the proposed hardware description, which we believe could ultimately realize information processing directly within the physical domain.

Code availability

The simulator code can be accessed on GitHub: <https://github.com/CipolliniDavide/FusedMemBrain.git>.

Acknowledgments

The authors are grateful to Karolina Tran for her insightful discussions on the potential of self-assembled materials, which greatly enriched this work. The authors acknowledge the International Workshop “Bio-inspired Information Pathways” by the CRC 1461 in collaboration with partners from CogniGron, as the event that inspired this research. The authors gratefully acknowledge the financial support from the Groningen Cognitive Systems and Materials Center (CogniGron). Partially funded by the Deutsche Forschungsgemeinschaft (DFG, German Research Foundation): Project MemTDE Project number 441959088 as part of the DFG priority program SPP 2262 MemrisTec Project number 422738993. D.C., L.S., and E.C. gratefully acknowledge the EUs Horizon 2020, from the MSCA-ITN-2019 Innovative Training Networks program “Materials for Neuromorphic Circuits” (MANIC) under the grant agreement No. 861153 for financial support.

References

- [1] E. Chicca, F. Stefanini, C. Bartolozzi, and G. Indiveri, “Neuromorphic electronic circuits for building autonomous cognitive systems”, *Proceedings of the IEEE*, vol. 102, no. 9, pp. 1367–1388, 2014. DOI: 10.1109/JPROC.2014.2313954.
- [2] D. Patterson, J. Gonzalez, Q. Le, C. Liang, *et al.*, “Carbon emissions and large neural network training”, *arXiv preprint arXiv:2104.10350*, 2021. DOI: 10.48550/arXiv.2104.10350.
- [3] M. M. Waldrop, “The chips are down for moore’s law”, *Nature News*, vol. 530, no. 7589, p. 144, 2016. DOI: 10.1038/530144a.
- [4] C. Mead, “How we created neuromorphic engineering”, *Nature Electronics*, vol. 3, no. 7, pp. 434–435, 2020. DOI: 10.1038/s41928-020-0448-2.
- [5] G. Indiveri, B. Linares-Barranco, T. J. Hamilton, A. v. Schaik, *et al.*, “Neuromorphic silicon neuron circuits”, *Frontiers in neuroscience*, vol. 5, p. 73, 2011. DOI: 10.3389/fnins.2011.00073.
- [6] D. Marković, A. Mizrahi, D. Querlioz, and J. Grollier, “Physics for neuromorphic computing”, *Nature Reviews Physics*, vol. 2, no. 9, pp. 499–510, 2020. DOI: 10.1038/s42254-020-0208-2.
- [7] M. Cotteret, H. Greatorex, A. Renner, J. Chen, *et al.*, “Distributed representations enable robust multi-timescale symbolic computation in neuromorphic hardware”, 2024. DOI: 10.48550/ARXIV.2405.01305.
- [8] S. A. McKee, “Reflections on the memory wall”, in *Proceedings of the 1st conference on Computing frontiers*, 2004. DOI: 10.1145/977091.977115.
- [9] E. Bullmore and O. Sporns, “Complex brain networks: Graph theoretical analysis of structural and functional systems”, *Nature reviews neuroscience*, vol. 10, no. 3, pp. 186–198, 2009. DOI: 10.1038/nrn2575.
- [10] A.-L. Barabási and R. Albert, “Emergence of scaling in random networks”, *science*, vol. 286, no. 5439, pp. 509–512, 1999. DOI: 10.1126/science.286.5439.509.
- [11] S. Micheloyannis, E. Pachou, C. J. Stam, M. Breakpear, P. Bitsios, M. Vourkas, S. Erimaki, and M. Zervakis, “Small-world networks and disturbed functional connectivity in schizophrenia”, *Schizophrenia research*, vol. 87, no. 1-3, pp. 60–66, 2006. DOI: 10.1016/j.schres.2006.06.028.
- [12] Y. Liu, M. Liang, Y. Zhou, Y. He, *et al.*, “Disrupted small-world networks in schizophrenia”, *Brain*, vol. 131, no. 4, pp. 945–961, 2008. DOI: 10.1093/brain/awn018.
- [13] M. A. Kramer, E. D. Kolaczyk, and H. E. Kirsch, “Emergent network topology at seizure onset in humans”, *Epilepsy research*, vol. 79, no. 2-3, pp. 173–186, 2008. DOI: 10.1016/j.eplepsyres.2008.02.002.
- [14] L. Wang, C. Zhu, Y. He, Y. Zang, Q. Cao, H. Zhang, Q. Zhong, and Y. Wang, “Altered small-world brain functional networks in children with attention-deficit/hyperactivity disorder”, *Human brain mapping*, vol. 30, no. 2, pp. 638–649, 2009. DOI: doi.org/10.1002/hbm.20530.
- [15] M. Barthélemy, “Spatial networks”, *Physics reports*, vol. 499, no. 1-3, pp. 1–101, 2011. DOI: 10.1016/j.physrep.2010.11.002.
- [16] X.-Y. Zhang, J. M. Moore, X. Ru, and G. Yan, “Geometric scaling law in real neuronal networks”, *Physical Review Letters*, vol. 133, no. 13, p. 138401, 2024. DOI: 10.1103/PhysRevLett.133.138401.
- [17] T. Dalgaty, F. Moro, Y. Demirağ, A. De Pra, G. Indiveri, E. Vianello, and M. Payvand, “Mosaic: In-memory computing and routing for small-world spike-based neuromorphic systems”, *Nature Communications*, vol. 15, no. 1, p. 142, 2024. DOI: 10.1038/s41467-023-44365-x.
- [18] A. Vahl, G. Milano, Z. Kuncic, S. A. Brown, and P. Milani, “Brain-inspired computing with self-assembled networks of nano-objects”, *Journal of Physics D: Applied Physics*, vol. 57, no. 50, p. 503001, 2024. DOI: 10.1088/1361-6463/ad7a82.
- [19] B. J. Kagan, A. C. Kitchen, N. T. Tran, F. Habibollahi, *et al.*, “In vitro neurons learn and exhibit sentience when embodied in a simulated game-world”, *Neuron*, vol. 110, no. 23, pp. 3952–3969, 2022. DOI: 10.1016/j.neuron.2022.09.001.
- [20] T. Isomura and K. Friston, “In vitro neural networks minimise variational free energy”, *Scientific reports*, vol. 8, no. 1, p. 16926, 2018. DOI: 10.1038/s41598-018-35221-w.
- [21] T. Isomura, K. Kotani, and Y. Jimbo, “Cultured cortical neurons can perform blind source separation according to the free-energy principle”, *PLoS computational biology*, vol. 11, no. 12, e1004643, 2015. DOI: doi.org/10.1371/journal.pcbi.1004643.
- [22] K. Friston, “The free-energy principle: A unified brain theory?” *Nature reviews neuroscience*, vol. 11, no. 2, pp. 127–138, 2010. DOI: /doi.org/10.1038/nrn2787.
- [23] C. Golgi, *Sulla fina anatomia degli organi centrali del sistema nervosa*. 1885.
- [24] M. Glickstein, “Golgi and cajal: The neuron doctrine and the 100th anniversary of the 1906 nobel prize”, *Current Biology*, vol. 16, no. 5, R147–R151, 2006. DOI: 10.1016/j.cub.2006.02.053.
- [25] G. E. Palade and S. Palay, “Electron microscope observations of intraneuronal and neuromuscular synapses”, *Anat. Rec.*, vol. 118, pp. 335–336, 1954.

- [26] E. G. Gray, “Axo-somatic and axo-dendritic synapses of the cerebral cortex: An electron microscope study”, *Journal of Anatomy*, vol. 93(Pt 4), pp. 420–33, 1959.
- [27] P. Burkhardt, J. Colgren, A. Medhus, L. Digel, *et al.*, “Syncytial nerve net in a ctenophore adds insights on the evolution of nervous systems”, *Science*, vol. 380, no. 6642, pp. 293–297, 2023. DOI: 10.1126/science.ade5645.
- [28] V. Thoma, S. Sakai, K. Nagata, Y. Ishii, *et al.*, “On the origin of appetite: GLWamide in jellyfish represents an ancestral satiety neuropeptide”, *Proceedings of the National Academy of Sciences*, vol. 120, no. 15, 2023. DOI: 10.1073/pnas.2221493120.
- [29] F. Pallasdies, S. Goedeke, W. Braun, and R.-M. Memmesheimer, “From single neurons to behavior in the jellyfish aurelia aurita”, *eLife*, vol. 8, 2019. DOI: 10.7554/eLife.50084.
- [30] H.-Z. Yuan, S. Shu, X.-D. Niu, M. Li, and Y. Hu, “A numerical study of jet propulsion of an oblate jellyfish using a momentum exchange-based immersed boundary-lattice Boltzmann method”, *Advances in Applied Mathematics and Mechanics*, vol. 6, no. 3, pp. 307–326, 2014. DOI: 10.4208/aamm.2013.m409.
- [31] H. O. Sillin, R. Aguilera, H.-H. Shieh, A. V. Avizienis, M. Aono, A. Z. Stieg, and J. K. Gimzewski, “A theoretical and experimental study of neuromorphic atomic switch networks for reservoir computing”, *Nanotechnology*, vol. 24, no. 38, p. 384 004, 2013. DOI: 10.1088/0957-4484/24/38/384004.
- [32] R. Zhu, S. Lilak, A. Loeffler, J. Lizier, A. Stieg, J. Gimzewski, and Z. Kuncic, “Online dynamical learning and sequence memory with neuromorphic nanowire networks”, *Nature Communications*, vol. 14, no. 1, 2023. DOI: 10.1038/s41467-023-42470-5.
- [33] G. Milano, G. Pedretti, K. Montano, S. Ricci, S. Hashemkhani, L. Boarino, D. Ielmini, and C. Ricciardi, “In materia reservoir computing with a fully memristive architecture based on self-organizing nanowire networks”, *Nature Materials*, vol. 21, no. 2, pp. 195–202, 2021. DOI: 10.1038/s41563-021-01099-9.
- [34] J. L. Rieck, D. Cipollini, M. Salverda, C. P. Quinteros, L. R. B. Schomaker, and B. Noheda, “Ferroelastic domain walls in BiFeO₃ as memristive networks”, *Advanced Intelligent Systems*, p. 2 200 292, 2022. DOI: 10.1002/aisy.202200292.
- [35] F. Profumo, F. Borghi, A. Falqui, and P. Milani, “Potentiation and depression behaviour in a two-terminal memristor based on nanostructured bilayer ZrO_x/Au films”, *Journal of Physics D: Applied Physics*, vol. 56, no. 35, p. 355 301, 2023. DOI: 10.1088/1361-6463/acd704.
- [36] J. B. Mallinson, J. K. Steel, Z. E. Heywood, S. J. Studholme, P. J. Bones, and S. A. Brown, “Experimental demonstration of reservoir computing with self-assembled percolating networks of nanoparticles”, *Advanced Materials*, p. 2402 319, 2024. DOI: doi.org/10.1002/adma.202402319.
- [37] T. Chen, J. van Gelder, B. van de Ven, S. V. Amitonov, *et al.*, “Classification with a disordered dopant-atom network in silicon”, *Nature*, vol. 577, no. 7790, pp. 341–345, 2020. DOI: 10.1038/s41586-019-1901-0.
- [38] F. Remacle, C. Collier, G. Markovich, J. Heath, U. Banin, and R. Levine, “Networks of quantum nanodots: The role of disorder in modifying electronic and optical properties”, *The Journal of Physical Chemistry B*, vol. 102, no. 40, pp. 7727–7734, 1998. DOI: 10.1021/jp9813948.
- [39] M. Liu, N. Yazdani, M. Yarema, M. Jansen, V. Wood, and E. H. Sargent, “Colloidal quantum dot electronics”, *Nature Electronics*, vol. 4, no. 8, pp. 548–558, 2021. DOI: 10.1038/s41928-021-00632-7.
- [40] H. Greateorex, O. Richter, M. Mastella, M. Cotteret, *et al.*, “TEXEL: A neuromorphic processor with on-chip learning for beyond-CMOS device integration”, 2024. arXiv: 2410.15854.
- [41] D. Cipollini and L. Schomaker, “Conduction and entropy analysis of a mixed memristor-resistor model for neuromorphic networks”, *Neuromorphic Computing and Engineering*, 2023. DOI: 10.1088/2634-4386/acd6b3.
- [42] G. S. Lynch, T. Dunwiddie, and V. Gribkoff, “Heterosynaptic depression: A postsynaptic correlate of long-term potentiation”, *Nature*, vol. 266, no. 5604, pp. 737–739, 1977. DOI: 10.1038/266737a0.
- [43] C.-W. Ho, A. Ruehli, and P. Brennan, “The modified nodal approach to network analysis”, *IEEE Transactions on Circuits and Systems*, vol. 22, no. 6, pp. 504–509, 1975. DOI: 10.1109/tcs.1975.1084079.
- [44] R. Pratap, V. Agarwal, and R. K. Singh, “Review of various available spice simulators”, in *2014 International Conference on Power, Control and Embedded Systems (ICPCES)*, 2014, pp. 1–6. DOI: 10.1109/ICPCES.2014.7062809.
- [45] K. Montano, G. Milano, and C. Ricciardi, “Grid-graph modeling of emergent neuromorphic dynamics and heterosynaptic plasticity in memristive nanonetworks”, *Neuromorphic Computing and Engineering*, vol. 2, no. 1, p. 014 007, 2022. DOI: 10.1088/2634-4386/ac4d86.
- [46] E. Miranda, G. Milano, and C. Ricciardi, “Modeling of short-term synaptic plasticity effects in ZnO nanowire-based memristors using a potentiation-depression rate balance equation”, *IEEE Transactions on Nanotechnology*, vol. 19, pp. 609–612, 2020. DOI: 10.1109/TNANO.2020.3009734.

- [47] R. S. Zucker and W. G. Regehr, “Short-term synaptic plasticity”, *Annual Review of Physiology*, vol. 64, no. 1, pp. 355–405, 2002. DOI: 10.1146/annurev.physiol.64.092501.114547.
- [48] Z. Wang, S. Joshi, S. E. Savel’ev, H. Jiang, *et al.*, “Memristors with diffusive dynamics as synaptic emulators for neuromorphic computing”, *Nature Materials*, vol. 16, no. 1, pp. 101–108, 2016. DOI: 10.1038/nmat4756.
- [49] A. Rodriguez-Fernandez, C. Cagli, J. Suñe, and E. Miranda, “Switching voltage and time statistics of filamentary conductive paths in HfO₂-based ReRAM devices”, *IEEE Electron Device Letters*, vol. 39, no. 5, pp. 656–659, 2018. DOI: 10.1109/LED.2018.2822047.
- [50] S. Menzel, S. Tappertzhofen, R. Waser, and I. Valov, “Switching kinetics of electrochemical metallization memory cells”, *Physical Chemistry Chemical Physics*, vol. 15, no. 18, p. 6945, 2013. DOI: 10.1039/c3cp50738f.
- [51] F. Caravelli, G. Milano, C. Ricciardi, and Z. Kuncic, “Mean field theory of self-organizing memristive connectomes”, *Annalen der Physik*, vol. 535, no. 8, 2023. DOI: 10.1002/andp.202300090.
- [52] G. Milano, F. Michieletti, C. Ricciardi, and E. Miranda, “Self-organizing neuromorphic nanowire networks are stochastic dynamical systems”, *Research Square*, 2024. DOI: <https://doi.org/10.21203/rs.3.rs-4102090/v1>.
- [53] L. Lapique, “Recherches quantitatives sur l’excitation électrique des nerfs traitée comme une polarisation”, *J. Physiol. Pathol.*, vol. 9, pp. 620–635, 1907.
- [54] D. J. Amit, *Modelling Brain Function: The World of Attractor Neural Networks*, 1st. 1992.
- [55] J. J. Hopfield, “Neural networks and physical systems with emergent collective computational abilities.” *Proceedings of the National Academy of Sciences*, vol. 79, no. 8, pp. 2554–2558, 1982. DOI: 10.1073/pnas.79.8.2554.
- [56] B. Poucet and E. Save, “Attractors in memory”, *Science*, vol. 308, no. 5723, pp. 799–800, 2005. DOI: 10.1126/science.1112555.
- [57] N. Qiao, H. Mostafa, F. Corradi, M. Osswald, F. Stefanini, D. Sumislawska, and G. Indiveri, “A reconfigurable on-line learning spiking neuromorphic processor comprising 256 neurons and 128k synapses”, *Frontiers in Neuroscience*, vol. 9, 2015. DOI: 10.3389/fnins.2015.00141.
- [58] M. Cotteret, H. Grotto, M. Ziegler, and E. Chicca, “Vector symbolic finite state machines in attractor neural networks”, *Neural Computation*, vol. 36, no. 4, pp. 549–595, 2024. DOI: 10.1162/neco_a_01638.
- [59] M. Barthélemy, *Spatial Networks: A Complete Introduction: From Graph Theory and Statistical Physics to Real-World Applications*. 2022. DOI: 10.1007/978-3-030-94106-2.
- [60] M. Barthélemy, “Crossover from scale-free to spatial networks”, *Europhysics Letters (EPL)*, vol. 63, no. 6, pp. 915–921, 2003. DOI: 10.1209/epl/i2003-00600-6.
- [61] M. Kaiser and C. C. Hilgetag, “Spatial growth of real-world networks”, *Phys. Rev. E*, vol. 69, p. 036103, 3 2004. DOI: 10.1103/PhysRevE.69.036103.
- [62] H. Jaeger, “The “echo state” approach to analysing and training recurrent neural networks-with an erratum note”, *Bonn, Germany: German National Research Center for Information Technology GMD Technical Report*, vol. 148, no. 34, p. 13, 2001.
- [63] W. Maass, P. Joshi, and E. D. Sontag, “Computational aspects of feedback in neural circuits”, *PLoS Computational Biology*, vol. 3, no. 1, e165, 2007. DOI: 10.1371/journal.pcbi.0020165.
- [64] J. Henseler and P. J. Braspenning, “Membrain: A cellular neural network model based on a vibrating membrane”, *International Journal of Circuit Theory and Applications*, vol. 20, no. 5, pp. 483–496, 1992. DOI: 10.1002/cta.4490200505.
- [65] T. W. Hughes, I. A. D. Williamson, M. Minkov, and S. Fan, “Wave physics as an analog recurrent neural network”, *Science Advances*, vol. 5, no. 12, 2019. DOI: 10.1126/sciadv.aay6946.